Building and Environment 112 (2017) 200–208

Contents lists available at ScienceDirect

Building and Environment

journal homepage: www.elsevier.com/locate/buildenv

Development of filter-free particle filtration unit utilizing condensational growth: With special emphasis on high-concentration of ultrafine particles

Juwon Pyo [a], Yoohyun Ock [a], Dongkyo Jeong [a], Kihong Park [b], Donggeun Lee [a, *]

[a] School of Mechanical Engineering, Pusan National University, Busan 46241, South Korea
[b] School of Environmental Science and Engineering, Gwangju Institute of Science and Technology (GIST), Gwangju 61005, South Korea

ARTICLE INFO

Article history:
Received 22 August 2016
Received in revised form
1 November 2016
Accepted 4 November 2016
Available online 4 November 2016

Keywords:
Condensational growth
Filter-free air purifier
High-volume flow rate
Indoor air quality
$PM_{2.5}$

ABSTRACT

The public health impact of particulate matter in ambient air with a size of 2.5 μm or smaller ($PM_{2.5}$) has been of great concern. It is well known that $PM_{2.5}$ is much more harmful to human health than coarse particles. To remove $PM_{2.5}$, most air purifiers on the market have been equipped with a high efficiency particulate air (HEPA) filter. Under the circumstances that generate $PM_{2.5}$ aerosols at high concentrations such as during indoor cooking or in work places, HEPA-grade filters are neither durable nor applicable because of their high replacement cost. Thus, a large number of cooks and workers are exposed to intensive emissions of $PM_{2.5}$ without proper filtration. In this paper, we introduce a novel concept to remove $PM_{2.5}$ without HEPA filters. A key idea is to use the condensational growth of particles. Once the particles have grown to a few micron, they are much easier to remove because of their increased inertia. Based on this, we developed the first prototype of a filter-free particle filtration unit consisting of an air saturator (equipped with water spray nozzles), a condenser in which humid air is cooled down to a supersaturation state and thereby allows particles to grow by condensation, and a multi-nozzle-impactor assembly for collecting the grown particles downstream of the condenser. We started with a small-scale model, and then demonstrated that a large-scale prototype could remove organic, inorganic, and metallic ultrafine particles with a collection efficiency of larger than 80% at a volume flow rate of 50–92 L/s.

1. Introduction

Airborne particles that are small enough to be inhaled have increasingly become a great concern in the world, because of their adverse health effects and environmental issues [1]. The US Environmental Protection Agency (EPA) has categorized these inhalable particles by size as PM_{10} and $PM_{2.5}$. PM_{10}, particles which have diameters of 10 μm and smaller, are relatively easy to remove because of their large inertia. Thus, they might be caught in the respiratory organs and coughed up via mucus and phlegm. In contrast, $PM_{2.5}$, fine particles which have diameters of 2.5 μm and smaller, tend to remain in the human body. Moreover, by penetrating the lower tissues of the respiratory tract or pulmonary alveoli, they can cause numerous serious diseases such as asthma, bronchitis, pneumonia, lung cancer, and heart attack [2]. Ultrafine particles in the $PM_{2.5}$ category with diameters smaller than 0.1 μm are often created by combustion at high concentrations of up to tens of millions of particles per 1 cm^3 [3,4]. Worse yet, these ultrafine particles include metal and organic chemicals and can grow into the coarse range of $PM_{2.5}$ by coagulation and condensation. As a result, their potential environmental and health risks become severely aggregated [5].

Ultrafine particles generated outdoors can also affect the quality of indoor air through the air intake of a building's HVAC system. HEPA filters, which are generally used in the indoor air purifiers on the market, are able to remove these ultrafine particles with high efficiency. However the annual HEPA filter replacement cost is approximately $100 [6] and can sometimes reach the price of the machine [7]. Of particular interest are small enclosed spaces such as indoor kitchens [8] and welding workshops [9], where ultrafine particles are generated at high concentrations. Workers in these areas could be directly exposed to such ultrafine particles unless

* Corresponding author.
E-mail address: donglee@pusan.ac.kr (D. Lee).

http://dx.doi.org/10.1016/j.buildenv.2016.11.011
0360-1323/

proper filtration or ventilation units are employed [10]. However, HEPA filter-based air purifiers are unlikely suitable for such environments because the filter replacement cycle can become much shortened with a large increase of pressure drop [11]. Therefore, it is necessary to develop a filter-free particle filtration unit that is capable of removing a high-concentration of ultrafine particles without HEPA filters.

A potential candidate for reaching this goal is an electrostatic precipitator (ESP) which is widely used for exhaust particle filtration in coal-fired power plants. However, even though the ESPs can be operated with a high collection efficiency and low pressure drop, they suffer from many unsolved problems. These include back-corona discharge and particle re-entrainment, which selectively occur depending on a particle's electrical resistivity; a low collection efficiency for sub-micrometer particles with a diameter range of 0.1–1.0 μm; and a low charging efficiency for ultrafine particles [12]. Moreover, in a modern ESP, the typical gas and particle residence time is 10–30 s, which is almost 100 times longer than that of residential air purifiers like those in our study. In other words, industrial ESPs are extremely large in size to increase the residence time and magnify the collection efficiency. Conversely, if the length of an ESP is shortened to below 0.1 m for residential applications, the collection efficiency will drop significantly. Indeed, it is not surprising that most of the residential air purifiers on the market are based on HEPA filters rather than ESPs.

In this study, we selected the use of water vapor condensation for ultrafine particles as an alternative filtration method without a HEPA filter, because it enables the growth of any type of ultrafine particle in the form of a water droplet within ~0.1 s [13]. Once ultrafine particles have grown to a few micrometers in diameter, the grown particles are relatively easy to remove, e.g. with simple impactors, because of their increased inertia [14]. Although the condensational growth of ultrafine particles has been extensively studied and is well described in a textbook [13], most of the previous researches has been performed on a small scale of less than l.0 L/s. As a result, there appeared a few commercial products utilizing the small-scale condensational growth; however, to the best of our knowledge, no large-scale device is available in the market.

For example, a condensation particle counter (CPC), which is one of the best-selling devices, has been demonstrated to enable the precise measurement of the number concentration of particles of any size through butanol vapor condensation. However, the CPCs are currently operated at a low gas flow rate of 0.017 L/s [15]. A particle-into-liquid sampler (PILS) [16], which is a well-known device that grows ultrafine bio-aerosol particles by water condensation, could successfully sample the enlarged particles from air with a water trap. However, the total operating gas flow rate was as low as 0.1 L/s. Only one study has demonstrated the large-scale condensational growth of ultrafine particles using water, which enabled an air flow of 42 L/s of air flow. The enlarged particles after the growth (which will be called “downstream particles” hereafter) were removed by either a micro-orifice impactor or virtual impactor [17]. Nevertheless, further improvement is required to commercialize such a system, because it requires a refrigerant-based cooling system installed in the condensation part in order to create a supersaturated state, resulting in high electricity consumption, and its collection efficiency was still as low as 53% at a fairly high supersaturation ratio of 2.48 (a saturator temperature of 29 °C vs a condenser temperature of 14 °C). The insufficient collection efficiency was attributed to the non-uniform growth of particles, but size measurements of the downstream particles were lacking.

Against this backdrop, the present study was emphasized on size measurements of the ultrafine particles upstream and downstream of a condenser where water vapor was supersaturated and particles grew by water vapor condensation. The reason for only testing ultrafine particles rather than the entire $PM_{2.5}$ range comes from the nature of condensational growth: in the condensing environment, if ultrafine particles are demonstrated to grow to 2 μm in diameter, initially larger particles should grow to more than 2 μm in diameter, and thus will undoubtedly be removed.

Based on this prospect, a small-scale prototype of a filter-free particle filtration unit was first prepared by combining an air saturator and a condenser. After experimental verification of the condensational growth of ultrafine particles, the design concept was extended to a large-scale filtration unit that included an air intake duct, a saturator equipped with a water spray nozzle, a heat exchanger-type condenser (as an option), a multi-nozzle-impactor assembly, and an induction fan. Three different types of ultrafine particles (inorganic, organic, and metallic) were tested to assess the condensing performance and collection efficiency of this prototype unit.

2. Methods

2.1. Theory of condensational growth

Humid air can be supersaturated upon cooling by any means. The supersaturation state is normally characterized by the ratio of the partial pressure of the condensing water vapor (P_∞) to its saturation water vapor pressure (P_s), called the supersaturation ratio (SSR): $SSR = P_\infty/P_s$. Under the supersaturation condition, particles begin to grow in size by water vapor condensation. The growth rate of particles strongly depends on the particle diameter (d_p) and SSR. A particle that is smaller than the mean free path of gas (λ) grows through irregular collisions with molecules corresponding to the free molecular regime, forming a liquid droplet that contains the particle. The growth rate of the droplet is given by Eq (1) [18]:

$$\frac{d(d_p)}{dt} = \frac{2M\alpha_c(p_\infty - p_d)}{\rho_p N_a \sqrt{2\pi m k T}}, \quad for\ d_p < \lambda \tag{1}$$

where M refers to the molecular weight of water; ρ_p is the density of the water droplet; α_c is a condensation coefficient for which a value of 0.04 is often used [18]; m is the mass of a single water molecule; k is Boltzmann's constant; N_a is Avogadro's number; T is the water vapor temperature; and P_d, the vapor pressure of water at the surface of a droplet, is slightly larger than P_s as a result of the surface curvature (Kelvin effect) [18]. Here, the droplet is assumed to be in a thermal equilibrium state with the surrounding gas.

When particles are larger than λ, they grow by the diffusion of water vapor into the surface, in accordance with the continuum regime calculated in Eq. (2):

$$\frac{d(d_p)}{dt} = \frac{4MD_v}{R\rho_p d_p T}(p_\infty - p_d), \quad for\ d_p > \lambda \tag{2}$$

where D_v represents the diffusion coefficient of the water vapor, and R is the gas constant. When a droplet grows to more than 300 nm, where the Kelvin effect is negligible, P_d gets closer to P_s, and Eq (2) is reduced to the following:

$$\frac{d(d_p)}{dt} = \frac{4MD_v}{R\rho_p d_p}\frac{p_s}{T}(SSR - 1) \tag{3}$$

Hence, particles can grow quickly in linear proportion to the SSR.

2.2. Small-scale experiment

2.2.1. General strategy and preparation

As a first step, a series of preliminary experiments were conducted to test the feasibility of condensational growth of ultrafine particles under low-concentration/low-flow rate conditions. For this small-scale experiment, a condensational growth unit was prepared by combining two parts in series: 1) a saturator equipped with a humidifier that saturates the air with water vapor, and 2) a condenser that cools the saturated air to a sufficient level for supersaturation.

Referring to Eqs. (1–3), one may notice that there are two important parameters for controlling the SSR and growth rate of particles: the saturator temperature (T_s) and condenser temperature (T_c). If the saturated air leaving the saturator at T_s is cooled to T_c in the condenser, the term of P_∞ in Eqs (1- 2) becomes a saturation vapor pressure of water at T_s as $P_s(T_s)$, whereas the P_d is approximately a saturation vapor pressure of water at T_c as $P_s(T_c)$, resulting in SSR = $P_s(T_s)/P_s(T_c)$. Because the P_s is very sensitive to temperature, a sufficiently large SSR could be obtained with a relatively small temperature difference ($\Delta T = T_s - T_c$).

To realize an economical (filter-free) particle filtration for $PM_{2.5}$ control, it is crucial to minimize the electricity consumption. Because cooling is much more expensive than heating, the condenser temperature (T_c) was set to either room temperature (20 °C) or the temperature (15 °C) of easily accessible tap water. The saturator temperature T_s was instead varied from 30 to 80 °C unless otherwise noted.

It is also interesting to verify whether the vapor condensation is applicable to any type of particles. Hence, two types of ultrafine particles were taken into account for the small-scale experiment: polydisperse inorganic particles of NaCl with a mean diameter of 54 nm, and monodisperse organic particles of polystylene latex (PSL) with a nominal diameter of 100 nm (Thermo Scientific). Each type of particle was generated using a spray drying method [19–21] and then fed into a saturator. The size distribution of ultrafine particles prior to the saturator was measured by a scanning mobility particle sizer (SMPS; Model 3936, TSI Corp).

2.2.2. A saturator and a condenser

The first saturator design was a home-made bubbler capable of supplying humid saturated air at 0.03 L/s; its temperature (T_s) was varied in the range of 60–80 °C. This humid air was mixed with the dry aerosol flow of NaCl or PSL at 0.0017 L/s and then fed into a condensing tube with a diameter of 1.27 cm maintained at 20 °C. Although this type is easy to realize in a laboratory, the mixing of two flows inevitably causes a humidity decrease of the saturated air by dilution. To minimize the dilution effect, the flow rate of saturated air was set to 18 times larger than that of the aerosol flow. As this was impractical in a large-scale experiment, the saturator was redesigned to be able to humidify air without mixing.

The second type of saturator included a small water chamber, in which an ultrasonic transducer is installed to produce micro droplets of water. An aerosol flow with NaCl or PSL particles is directly connected to the chamber, which allows not only to carry the water droplets at higher volume flow rates but also to facilitate water evaporation due to enlarged surface area. As a result, 100% saturation was simply attained with 0.017 L/s of aerosol flow at T_s = 30 °C. The outlet of this saturator was connected to the same condensing tube maintaining at 20 °C.

During cooling of humid aerosol flow in the condensing tube, the particles are expected to grow to a few micron by condensation. The size distribution of enlarged particles downstream of the condenser was measured by an optical particle sizer (OPS; Model 3330, TSI Corp).

2.3. Large-scale experiment

The large-scale experiment was conducted with focus on experimental verifications of condensational growth and subsequent filtration of high-concentration particles at high flow rates. Fig. 1 illustrates the experimental setup of the filter-free particle filtration unit which is mainly composed of a saturator, a condenser, and a removal device. Design and instrumentation of each component will be described in the following subsections.

2.3.1. A large-scale saturator

Unlike in the small-scale experiment, neither the bubbler nor the supersonic transducer was effective for saturating the air 100% in the large-scale experiment. A nozzle was used to spray the water directly into the aerosol flow. For the nozzle installation, an 80- cm long rectangular duct system with a square throat (30 cm × 30 cm) was fabricated using transparent acrylic plates. One end of this duct was used as an indoor air intake. A heating coil was also installed 15 cm from the inlet. The water spray nozzle was installed 50 cm from the air intake and sprayed water droplets toward the incoming air. Next, a condenser, a removal device, and an air-suction fan were sequentially installed at the other end of the duct.

The spray nozzle operated fairly well with a 0.2 mm opening and 3 bar of injection pressure. The supply rate of the water (m_{H2O}) needed to achieve saturation of the aerosol flow can be calculated using Eq (4).

$$(P_s - P_{in})Q = m_{H2O}RT_s \tag{4}$$

where P_{in} is the partial pressure of the water vapor at the air intake

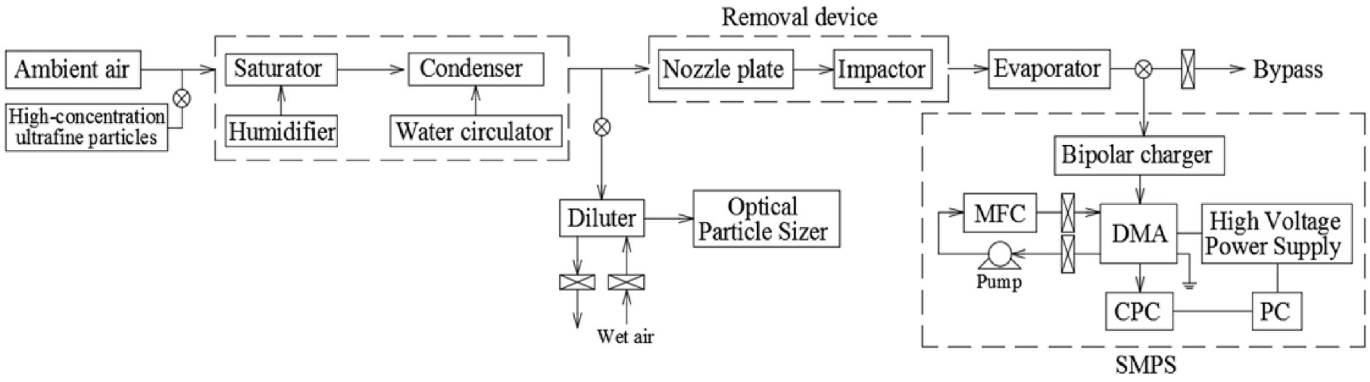

Fig. 1. An experimental setup of the present filter-free air purifier employing a plate heat exchanger condenser and its performance test.

that can be calculated based on the relative humidity (RH) measurement; P_s is again the saturation vapor pressure of the water at the saturator temperature (T_s); and Q is the volume flow rate of the aerosol flow, which ranges from 50 to 92 L/s. For example, the minimum value of m_{H2O} required to saturate dry air (RH = 15%) at 50 L/s is calculated to be ~1.4 g/s. Based on this, a series of preliminary tests were conducted while controlling the heating coil and varying the nozzle size. As a result, the temperature and relative humidity of the air right ahead of the condenser could be controlled to be 30 °C and more than 95%, respectively. At that moment, the actual amount of spraying water was approximately 1.7 g/s, indicating that the sprayed droplets did not completely evaporate.

2.3.2. A large-scale condenser equipped with heat-exchanger

The first condenser design of the large-scale was a type of cross-flow flat-plate heat exchanger [22,23], consisting of nineteen thin aluminum flat plates (30-cm high and 24-cm long). These plates were stacked vertically (not on top of each other) in a rigid rack, and aligned parallel to each other at equal intervals of 1.5 cm, allowing humid air (at 30 °C) and tap water (15 °C) to flow through the channels formed by the plates. These fluids flowed into alternating channels. Thus the air and water never mixed but exchanged heat. By allowing the water to flow from the top to bottom, the humid air flowing horizontally could be cooled along the duct, resulting in a supersaturation state. Because of the large inter-planar spacing, the pressure loss across the condenser was as low as 100 Pa.

The cooling performance of the plate heat exchanger was tested by measuring the air temperature at five different axial positions along an air-flow channel in the middle of the heat exchanger. Moreover, corresponding local temperatures of air and water were calculated for the heat exchanger using a commercial code Fluent 16 and then compared with the measured temperatures.

To assess the vapor-condensing performance of this condenser, high-concentration ultrafine particles (will be described more in Section 2.3.5) were released in between the saturator and the condenser. A small fraction of the enlarged particles downstream of the condenser was sampled and then diluted for further in-situ measurement of the size distribution using the OPS, as depicted in Fig. 1.

2.3.3. A large-scale removal device

The enlarged particles downstream of the condenser were removed by a removal device (circular-jet impactors), which consisted of four-hundred converging nozzles with 1.5 mm openings paired with the same number of small cylindrical columns, as schematically shown in Fig. 2. The collection efficiency of these impactors is well characterized by a cut-off size (d_{50}), which represents the minimum diameter of removable particles. The nozzle size (D_j = 1.5 mm) was determined to have a sufficiently small value of d_{50} (= 0.9 μm) at Q = 50 L/s using Eq (5).

$$d_{50} = \left[\frac{9\eta D_j(Stk_{50})}{\rho_p U}\right]^{1/2} \quad (5)$$

where Stk_{50} is the Stokes number corresponding to 50% of the cumulative collection efficiency and often approximated as 0.25 for circular-jet impactors [17], U is the average nozzle exit velocity, and the humid air viscosity (η) is 1.82×10^{-5} kg/m•s.

The design performance of the nozzle-impactor assembly was tested by the following procedure. Commercial coarse particles (PTFE, Polytetrafluoroethylene, TP-214) with 2–4 μm in diameter were sprayed as the upstream particles in the 1 m^3 test chamber, and the nozzle-impactor assembly with an air intake and a fan was positioned in the middle of the chamber and operated with 50 L/s. A tube with 1.27 cm diameter connected to the OPS was inserted to sample the particles near the fan exhaust, and then the transient variation in size distribution of particles in the chamber was monitored continually for 10 min after turning on the fan.

2.3.4. A compact condenser-impactor assembly

This section is devoted to address how to shorten the total length of the condenser and removal device. Special emphasis should be placed on that air flowing through a nozzle essentially undergoes an adiabatic expansion and cooling [24,25]. This implies that the nozzle could play a double role as an alternative condenser

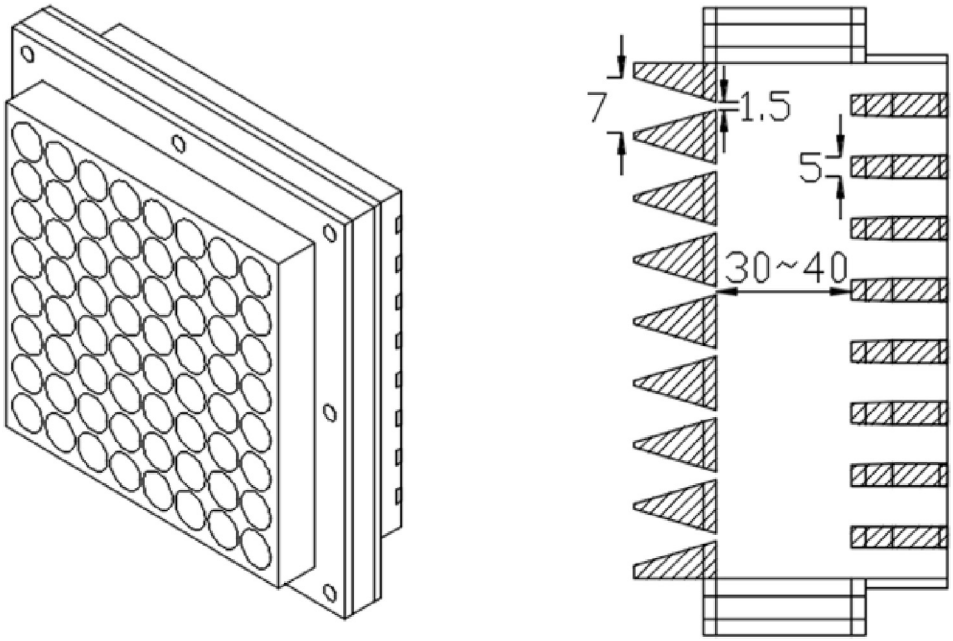

Fig. 2. A schematic design of adiabatic expansion nozzle and impactor.

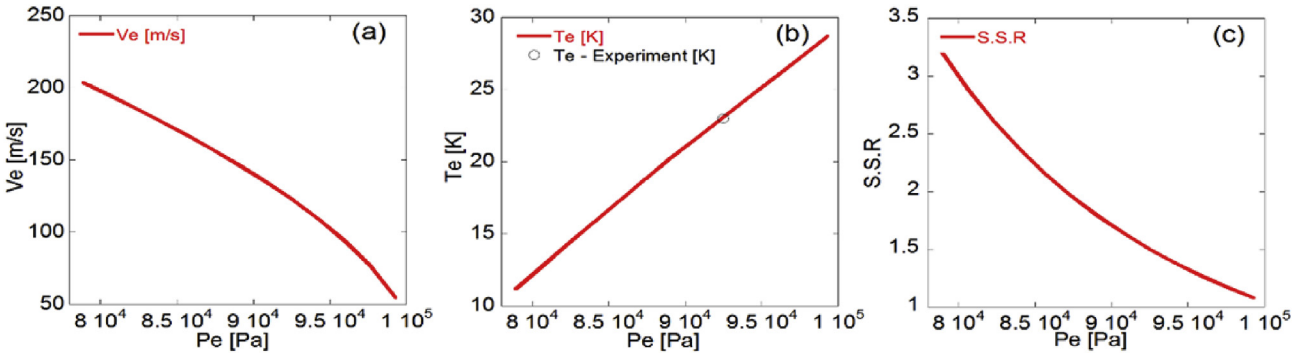

Fig. 3. Simple model predictions of (a) velocity, (b) temperature, and (c) SSR of humid air at the nozzle exit as a function of downstream pressure.

with the shortest length and as a part of removal device for accelerating the particles toward the impactors. Therefore, this allows to eliminate the heat exchanger and to use the nozzle-impactor assembly alone for growing and removing ultrafine particles simultaneously. This is a compact condenser-impactor assembly.

As the extent of adiabatic cooling is a key element for determining the nozzle feasibility, the velocity (V_e) and temperature (T_e) of air at the nozzle exit were calculated by the well-known isentropic expansion formula for ideal gas and thermodynamic enthalpy conservation in open system as follows:

$$V_e = \sqrt{\frac{2\gamma}{\gamma-1}RT_i\left[1-\left(\frac{P_e}{P_i}\right)^{\frac{\gamma}{\gamma-1}}\right]+V_i^2} \tag{6}$$

$$T_e = T_i - \frac{1}{2C_p}\left(V_e^2 - V_i^2\right), \tag{7}$$

where the subscript i and e represent the states upstream and downstream of the nozzle. In the equations, V, P, and T refer to velocity, pressure, and temperature of humid air; and C_p, γ, and R refer to specific heat at constant pressure, specific heat ratio, and gas constant of air, respectively. The upstream properties of the saturated humid air were approximated by those of dry air: $C_p = 1007$ J/kg•K; $\gamma = 1.4$; $V_i = 1$ m/s at $Q = 92$ L/s; $P_i = 1$ atm.

Based on these properties and nozzle design in Fig. 2, the velocity (V_e), temperature (T_e), and supersaturation ratio (SSR) of humid air at the nozzle exit were calculated as a function of exit pressure of nozzle (P_e) by Eqs. 6–7 and showed in Fig. 3-(a), 3-(b), and 3-(c), respectively. The result suggests that upon decreasing P_e at a constant P_i, the air was gradually accelerated at the expense of its enthalpy, resulting in a gradual decrease in its temperature and increase in SSR.

Referring to Fig. 3-(c) and Eq (3), the exit pressure P_e should be lowered at least below 90 kPa, resulting in SSR > 1.75 which ensures the ultrafine particles to grow beyond 1 μm. With the fan used for the heat exchanger-installed system (50 L/s), the downstream pressure of nozzle was never decreased below 98 kPa. To solve this problem, the fan was replaced with a high-capacity fan operating with a larger discharging volume (92 L/s). With this, upstream pressure of the fan was measured to ~93 kPa, 8 kPa lower than the atmospheric pressure. By approximating the P_e with this measured value, the T_e and SSR were obtained to 23 °C and 1.5 from the curves in Fig. 3-(b) and 3-(c), respectively.

2.3.5. Collection efficiency of the filter-free particle filtration unit

For the large-scale experiments, two different types of polydisperse ultrafine particles were used: the inorganic NaCl particles with a mean diameter of 54 nm and metallic Ag particles with a mean diameter of 25 nm produced by an evaporation-condensation method [26]. There are two distinct reasons for the use of Ag particles instead of PSL particles: 1) the Ag particles are produced at the highest concentration; 2) they are metallic. In contrast, PSL particles, typically used as an expensive size standard with a low gas flow rate, are provided as a dilute (1%) colloidal suspension. Thus, PSL particles, if introduced to the system operating at 50 L/s or higher, would be too much diluted for high-concentration test of the system. In addition, metallic particles have not been tested yet.

After passing through the removal device, a fraction of the remaining particles (still in a form of droplet) were sampled and then dried by an evaporator (in Fig. 1) consisting of a tubular electric furnace (Type F21100, Barnstead Thermolyne Corp.) and a diffusion dryer (with silica gel). The size distributions of the dried particles (also called the downstream particles of the system) were measured in terms of $dN/d\log(d_p)$ by SMPS and then compared with those of the upstream particles measured at the system inlet. Note that the SMPS-returned $dN/d\log(d_p)$, after being multiplied by a constant size bin in logarithmic scale ($\Delta\log(d_p) = 0.095$), indicates the number concentration of particles in a size range of $\log(d_p)$ and $\log(d_p) + \Delta\log(d_p)$ [27]. Thus, the collection efficiency (η) of the system is obtained as a function of size simply by comparing the size distributions between the downstream and upstream particles as shown in Eq (8).

$$\eta = 1 - \frac{(dN/d\log d_p)_e}{(dN/d\log d_p)_i} \tag{8}$$

where the subscript i and e represent the upstream and downstream of the system.

Some of the particles might be unintentionally lost in the system; for instance, particles might have been caught and removed by the sprayed droplets, like in a scrubbing system. In order to eliminate this concern, the spray nozzle and air heater, after being taken out of the system, were installed and operated inside the 1-m^3 test chamber, similar to conducting a test in a constant-temperature and constant-humidity chamber. The chamber was then connected to the present filter-free particle filtration unit without the saturator. Under these circumstances, after the temperature and humidity in the chamber reached 30 °C and 100%, respectively, the same system performance measurement was repeated. It was confirmed that the unintended particle loss in the saturator was negligible. Further details of the instrumentation used for the particle generation and measurements are available in our previous publications [19–21,26].

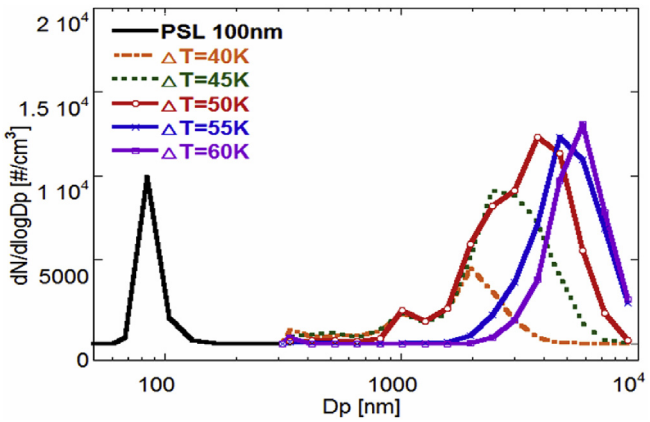

Fig. 4. Lab-scale condensational growth using bubbling-type saturator.

3. Results and discussion

3.1. Small-scale experiment for condensational growth

As described in Section 2.2, the first feasibility test for condensational growth was conducted with the assembly of bubbler-type saturator and tubular condenser. Fig. 4 shows the variations in size distribution of the monodisperse 100-nm PSL particles along with their controlled condensational growth. When the saturator temperature (T_s) was increased at a fixed condenser temperature (T_c) of 20 °C, the narrow size distribution curve of the PSL particles upstream of the condenser steadily shifted to larger sizes as a result of the condensation, indicating that the condensation and growth were accelerated, as expected, by increasing the temperature difference ($\Delta T = T_s - T_c$) and thereby the SSR. Fig. 4 also shows that the 100-nm PSL particles grew to 2 μm or greater when $\Delta T \geq 45$ °C, exceeding the target size, although the size distributions were relatively widened. This may have resulted from the inhomogeneous mixing of the saturated air flow and aerosol flow of the ultrafine particles: 0.03 L/s vs 0.0017 L/s. It is also speculated that the self-nucleation of the supersaturated water vapor followed by rapid coagulation between the water nuclei might have occurred, along with non-uniform condensation, leading to the broadening of the size distributions. This sounds plausible because 1) the SSR of the humid air excessively increases at $\Delta T \geq 45$ °C; 2) the total number concentration of particles is clearly increased with the temperature difference, as shown in Fig. 4, which is a sign of nucleation creating new particles.

Because the nucleation requires excessive energy consumption for heating the saturator in this study, the second saturator design (ultrasonic transducer) for energy efficient humidification was tested using emphasis on minimizing the nucleation. Given $T_s = 30$ °C, Q = 0.016 L/s, and a residence time in the condensing tube of 0.45 s, the 54-nm polydisperse NaCl particles were successfully grown to a size greater than 2 μm only with $\Delta T = 10$ °C as shown in Fig. 5. Note that the total number concentration is slightly increased from 4500 to 5500 #/cm^3, by 22% that is much lower than the increase (>100%) in the case of PSL particles (refer to Fig. 3). This suggests that nucleation is likely minimized to some degree as intended.

3.2. Large-scale experiment

3.2.1. A heat exchanger-installed condenser: air cooling and condensational growth

Referring to Section 2.3.2, humid air temperature was measured along the plate heat exchanger and compared with the numerical simulation result. Fig. 6 shows that the measured air temperatures were all in good agreement with the predicted temperature profile. Based on the cooling characteristics, and with the goal of downsizing the device, the length of the heat exchanger could be shortened to 10 cm, because the air temperature had already dropped sufficiently by 12 °C in the first 10 cm section, producing a high SSR (~2.0).

Based on the SSR, ultrafine particles are expected to grow by condensation even with a large air flow rate of 50 L/s. To confirm this, the size distribution of enlarged NaCl particles downstream of the condenser was measured using the OPS. Fig. 7 shows that with a residence time 0.2 s, most of the upstream NaCl particles with a mean diameter of 54-nm in the present unit grew by more than 1 μm to a size of up to 10 μm, beyond the cut-off diameter (d_{50} = 0.9 μm) of the subsequent impactors. It is also confirmed from Fig. 7 that the condensation takes place so stably that the resultant size distribution is quite reproducible through three repetitive experiments; the maximum variation of the measurement was as low as 5.7% in a range of 1.0–5.0 μm.

3.2.2. A removal device: collection efficiency for commercial coarse particles

As described in Section 2.3.3, the particle removal device, that is the multi nozzle-impactor assembly, was prepared to collect coarse particles grown in the upstream part (condenser), and designed to exhibit a cut-off diameter of 0.9 μm with air flow rate of 50 L/s. To

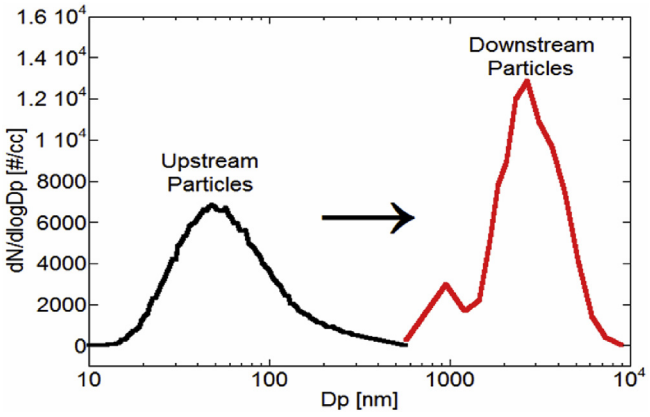

Fig. 5. Condensational growth of ultrafine particles using ultrasonic transducer saturator.

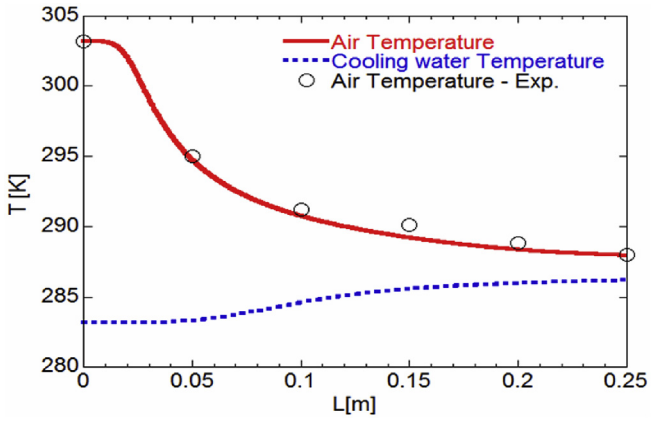

Fig. 6. Comparison of temperature profiles between experiment and simulation inside the gas flow channel of the water-cooled heat exchanger.

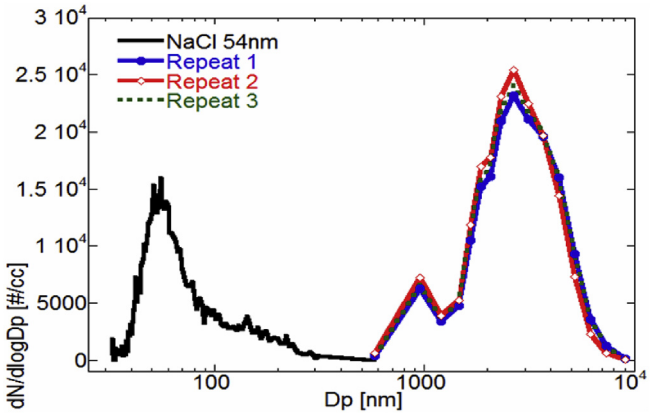

Fig. 7. Demonstration of condensational growth of ultrafine particles using water-cooled heat exchanger condenser at a high volume flow rate.

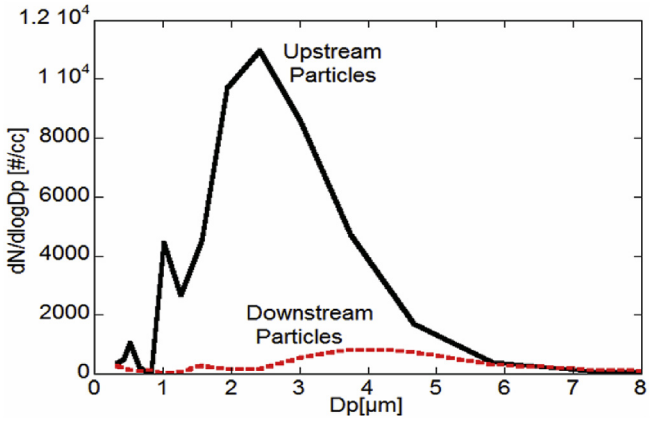

Fig. 8. Comparison of size distribution of coarse PTFE particles before and after the removal by multi nozzle-impactor assembly.

assess its collection efficiency as a function of size (referring to Eq (8)), the performance test of the removal device was conducted in accordance with the procedure in Section 2.3.3: by monitoring commercial micron PTFE particles in the chamber.

Fig. 8 shows the size distribution of the micron particles that remain (not removed yet) in the chamber after 10-min operation of the device, in comparison with their initial size distribution. It is found that number concentrations of the micron particles are sharply decreased only in 10 min, in a range of 1–4 μm. Based on the data, the collection efficiency of the removal device are calculated as a function of size by Eq (8) and summarized in Table 1. The collection efficiency is maintained high (>93%) in a range of 1–3 μm, but decreases for larger particles (>4 μm).

One peculiar point that should be noted is that the present impactors were not effective at removing particles larger than 4 μm, compared with the smaller ones, which seemed to contradict the impaction principle. It is however noted that the measured collection efficiency is not the single-pass particle filtration efficiency of our removal device, but denotes the overall effectiveness of reducing indoor particle concentrations [28]. In case of imperfect design and/or positioning of air intake and fan exhaust, some part of fan discharge air could be separated from the main recirculation stream, forming a vortex near the inlet and outlet of the device. Then, large particles, that tend to deviate from air stream, have less chance to enter the air intake, compared to smaller particles. This might cause the performance degradation of the removal device for particles >4 μm.

3.2.3. *Overall collection efficiency: for the entire unit incorporating heat exchanger*

The present filter-free air purifier was finally realized by integrating the air intake duct holding the saturator, condenser, nozzle-impactor assembly, and fan (see Fig. 1; for details, refer to Section 2.3.5). To assess the overall collection efficiency of the heat exchanger-installed filtration unit, NaCl particles of 54 nm were again released in between the saturator and condenser. Most of the particles grown by condensation were eliminated by 400 nozzles and impactors; however, there were still a small fraction of the particles that passed through the impactor safely.

The size distribution of the surviving particles, after being dried, was measured using the SMPS and shown with a dotted line in Fig. 9. Their size distribution was measured twice and was reproducible. The solid line in the figure represents the size distribution of the NaCl particles measured at the same position, but without spraying water (preventing the condensation). As expected from Figs. 7 and 8, the results demonstrated that major part of ultrafine particles in a range of 40–80 nm are successfully removed from the air without HEPA filter, resulting in large decreases of number concentrations in the size range. The corresponding collection efficiency is calculated by Eq (8) and shown in Table 1. The collection efficiency is high (above 90%) for particles smaller than 70 nm, whereas the efficiency for larger particles appears to decrease slightly with fluctuations. This might be attributed to the less population of larger particles which tend to be vulnerable to systematic disturbance.

Table 1
The collection efficiency of the removal device alone and the entire filtration unit incorporating two types of condensers.

Collection Efficiency					
PTFE particles (Fig. 8)		NaCl particles (Fig. 9)		Ag particles (Fig. 10)	
d_p [nm]	Collection Efficiency [%]	d_p [nm]	Collection Efficiency [%]	d_p [nm]	Collection Efficiency [%]
1007	98.9	32.4	99.4	10.6	99.8
1254	97.3	35.6	99.3	15.1	93.6
1562	93.9	40.1	97.9	20.2	91.8
1944	98.2	45.2	98.3	24.1	91.2
2421	98.4	50.9	97.7	31.1	94.3
3014	93.5	55.0	97.0	34.6	94.9
3753	82.7	60.9	94.6	41.4	95.6
4672	56.4	65.0	93.3	46.1	94.8
		71.1	89.2	51.4	94.0
		76.4	87.4	55.2	93.3
		80.2	84.3	61.5	90.7
		91.1	81.7	66.1	88.6
				71.0	87.0

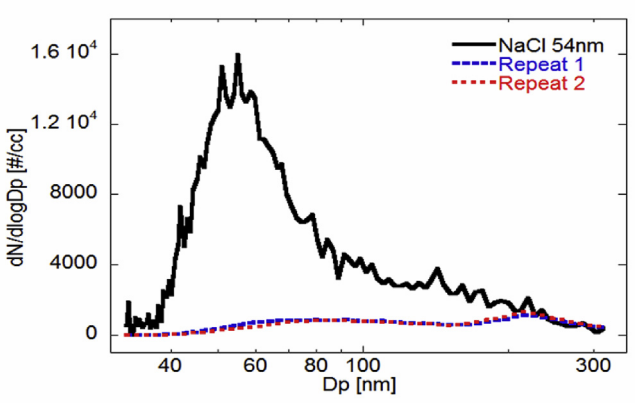

Fig. 9. Comparison of size distribution of ultrafine particles with and without operation of humidifier; upon operating plate heat exchanger condenser, nozzle-impactor assembly, evaporator, and SMPS.

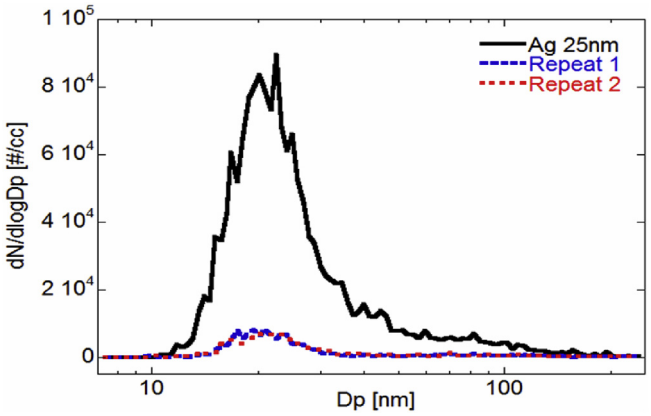

Fig. 10. Comparison of size distribution of ultrafine metallic particles with and without operation of humidifier, upon use of adiabatic-expansion condensers, inertial impactors, evaporator, and SMPS.

3.2.4. Overall collection efficiency: for the entire unit using adiabatic cooling

In this section, the second version of the present filtration unit using an adiabatic cooling through nozzles will be discussed. Prior to analysis of the collection efficiency, let us recall Section 2.3.4 where water vapor condensation and growth rate were concluded to be controlled by adjusting the nozzle exit pressure P_e. Fig. 3-(c) and Eq (3) indicates that the P_e should be lowered at least below 90 kPa, in order to obtain SSR > 1.75 making the ultrafine particles grow beyond 1 μm. With the fan used for the system equipped with the heat exchanger (50 L/s), the downstream pressure of nozzle was never decreased below 98 kPa. To solve this problem, the fan is replaced by a high-capacity fan that operated with a larger discharge volume (92 L/s). With this, upstream pressure of the fan is measured at ~93 kPa, which was 8 kPa lower than the atmospheric pressure. By approximating P_e using this measured value, T_e and SSR values of 23 °C and 1.5 were obtained from the curves in Fig. 3-(b) and 3-(c), respectively.

Although the approximation sounds reasonable, the true value of P_e at the nozzle throat more likely differ from the pressure measured between the nozzle exit and the impactor. In other words, the air begins to decelerate right after departing the nozzle exit, which in turn recovers the air pressure to some degree. Hence, the real local exit pressure of P_e could be lower than 93 kPa, suggesting that the estimation provides a lower limit for the SSR, i.e., the true SSR is ≥1.5. Although it is necessary to measure the size of particles downstream of the nozzles, this could not be done. Because the OPS was not powerful enough to draw the air by overcoming the negative pressure. Nevertheless, ultrafine particles carried by saturated air are believed to grow through the nozzle.

With the large fan, saturated humid air at 30 °C and metallic Ag particles of 25 nm at high concentration are drawn to this compact system. As in the case of the system equipped with the heat exchanger, the overall collection efficiency is likewise measured using the SMPS after drying the particles that have passed through the removal device. Fig. 10 shows that the upstream Ag particles, which are denoted with a solid line, were effectively removed by the system, leaving behind only a low level of particles. Here, the term of upstream represents the particles passing through the system without spraying water, i.e., no condensation and no removal. As shown in the third column of Table 1, the overall collection efficiency is found to >87% in the entire range of 10–70 μm. These data are comparable to those of heat exchanger-installed system in Table 1, which suggests that the concept of condensational growth by adiabatic cooling is working and the compact design of condenser-remover assembly is clearly helpful for minimizing the length of the entire system. However, use of too small nozzles is not desirable because it could cause a significant decrease in air flow rate: this in turn requires a larger-capacity fan so that noise will become an issue.

3.2.5. Potential and limitations of the present filter-free particle filtration unit

As stated in the preceding subsections, the present filter-free particle filtration unit has great potential to be the best solution for removing ultrafine particles at high concentrations. However, it should be noted that there are some areas of improvements for commercialization. Particularly for home use, the greatest concern would be the noise (≥80 dB) from the large-capacity fan for operation of the adiabatic cooling nozzles. Further optimization of nozzles should be continued in a way of reducing the fan capacity and the noise to the acceptable levels (e.g., <40 dB at night). The heat-exchanger installed system could circumvent the noise issue, however it will require additional cooling water supply. If a direct tap water line is considered to connect to the system, the present filtration unit could be used as a built-in accessory in a kitchen. Another issue would be the large size of the present system relative to conventional residential air purifiers. The saturator that is the largest part of the system should be redesigned to have a minimal (or adaptable) length; for example, smaller water-spray nozzles or higher spray pressure might be an option.

Upon taking these issues into account, the present unit is believed particularly suited to hot and humid circumstances such as combustion exhaust, because the exhaust air essentially holds high humidity enough to grow the particles by condensation; and this eliminates the need of the saturator. This offers another opportunity to reduce the length of the system.

4. Conclusions

In this study, we proposed the novel idea of practically removing ultrafine particles without HEPA-grade filter using condensational particles growth, while simultaneously increasing the particles' inertia. The small-scale experiment revealed that 10 °C cooling of humid air was sufficient for the rapid condensational growth of ultrafine particles. Based on this, we successfully designed two types of condensers: 1) a plate heat exchanger that used tap water as a coolant and 2) a system that used 400 isentropic cooling nozzles with no need for an external coolant. Through a series of analyses and experiments, we demonstrated that inorganic 54-nm

NaCl particles and organic PSL 100 nm particles grew rapidly to 2–5 μm. An integrated device of nozzle and impactor with a cut off size of 0.9 μm was also designed for removing the large particles grown by condensation. Finally, the present filter-free particle filtration unit was proved to be effective for treating inorganic, organic, and even metallic ultrafine particles with an acceptable collection efficiency of >81%.

Acknowledgements

This work was supported by the National Research Foundation (No. 2014M3C8A5030614), and also by the National Research Foundation (No. 2016R1A2B2014141).

References

[1] N.A. Greene, V.R. Morris, Assessment of public health risks associated with atmospheric exposure to PM2.5 in Washington, DC, USA, Int. J. Env. Res. Pub. He 3 (2006) 86–97.
[2] A.D. Maynard, E.D. Kuempel, Airborne nanostructured particles and occupational health, J. Nanopart. Res. 7 (2005) 587–614.
[3] O. Sippula, J. Hokkinen, H. Puustinen, P. Yli-Pirilä, J. Jokiniemi, Comparison of particle emissions from small heavy fuel oil and wood-fired boilers, Atmos. Environ. 43 (2009) 4855–4864.
[4] L.S. Johansson, C. Tullin, B. Leckner, P. Sjövall, Particle emissions from biomass combustion in small combustors, Biomass. Bioenerg. 25 (2003) 435–446.
[5] M. Hallquist, J.C. Wenger, U. Baltensperger, Y. Rudich, D. Simpson, M. Claeys, J. Dommen, N.M. Donahue, C. George, A.H. Goldstein, J.F. Hamilton, H. Herrmann, T. Hoffmann, Y. Iinuma, M. Jang, M.E. Jenkin, J.L. Jimenez, A. Kiendler-Scharr, W. Maenhaut, G. McFiggans, T.F. Mentel, A. Monod, A.S.H. Prévôt, J.H. Seinfeld, J.D. Surratt, R. Szmigielski, J. Wildt, The formation, properties and impact of secondary organic aerosol: current and emerging issues, Atmos. Chem. Phys. 9 (2009) 5155–5236.
[6] W.J. Fisk, D. Faulkner, J. Palonen, O. Seppanen, Performance and costs of particle air filtration technologies, Indoor Air 12 (2002) 223–234.
[7] Consumer Reports; Air Purifier Buying Guide, 2016. http://www.consumerreports.org/cro/air-purifiers/buying-guide.htm/.
[8] L.A. Wallace, S.J. Emmerich, C. Howard-Reed, Source strengths of ultrafine and fine particles due to cooking with a gas stove, Environ. Sci. Technol. 38 (2004) 2304–2311.
[9] P. Brand, K. Lenz, U. Reisgen, T. Kraus, Number size distribution of fine and ultrafine fume particles from various welding processes, Ann. Occup. Hyg. 57 (2012) 305–313.
[10] R. Mostofi, B. Wang, F. Haghighat, A. Bahloul, L. Jaime, Performance of mechanical filters and respirators for capturing nanoparticles —Limitations and future direction, Ind. Health 48 (2010) 296–304.
[11] C. David Cooper, F.C. Alley, Air Pollution Control: a Design Approach, (second ed.), Waveland Press, 2002, pp. 547–561, pp. 99–238.
[12] A. Jaworek, A. Krupa, T. Czech, Modern electrostatic devices and methods for exhaust gas cleaning: a brief review, J. Electrostat 65 (2007) 133–155.
[13] S.K. Friedlander, Smoke, Dust, and Haze; Fundamentals of Aerosol Behavior, (second ed.), Oxford University Press, New York, 2000, pp. 249–257.
[14] V.A. Marple, K. Willeke, Impactor design, Atmos. Environ. 10 (1967) 891–896.
[15] M.R. Stolzenburg, P.H. McMurry, An ultrafine aerosol condensation nucleus counter, Aerosol. Sci. Tech. 14 (1991) 48–65.
[16] D.A. Orsini, Y. Ma, A. Sullivan, B. Sierau, K. Baumann, R.J. Weber, Refinements to the particle-into-liquid sampler (PILS) for ground and airborne measurements of water soluble aerosol composition, Atmos. Environ. 37 (2003) 1243–1259.
[17] P. Demokritou, T. Gupta, P. Koutrakis, A high volume apparatus for the condensational growth of ultrafine particles for inhalation toxicological studies, Aerosol. Sci. Tech. 36 (2002) 1061–1072.
[18] W. C. Hinds, Aerosol Technology: Properties, Behavior, and Measurement of Airborne Particles, (second ed.), John Wiley & Sons, Los Angeles, CA, 1999, pp. 278–292.
[19] R. Zahaf, J. Jung, Z. Coker, S. Kim, T. Choi, D. Lee, Pt catalyst over SiO_2 and Al_2O_3 supports synthesized by aerosol method for HC-SCR $DeNO_x$ application, Aerosol. Air. Qual. Res. 15 (2015) 2409–2421.
[20] D. Lee, K. Park, M.R. Zachariah, Determination of the size distribution of polydisperse nanoparticles with single-particle mass spectrometry: the role of Ion kinetic energy, Aerosol. Sci. Tech. 39 (2005) 162–169.
[21] H. Lee, T.J. Kim, C. Li, I.D. Choi, Y.T. Kim, Z. Coker, T.-Y. Choi, D. Lee, Flame aerosol synthesis of carbon-supported Pt–Ru catalysts for a fuel cell electrode, Int. J. Hydrogen. Energ 39 (2014) 14416–14420.
[22] B. Prabhakara Rao, P. Krishna Kumar, S.K. Das, Effect of flow distribution to the channels on the thermal performance of a plate heat exchanger, Chem. Eng. Process 41 (2002) 49–58.
[23] C. Zhan, X. Zhao, S. Smith, S.B. Riffat, Numerical study of a M-cycle cross-flow heat exchanger for indirect evaporative cooling, Build. Environ. 46 (2011) 657–668.
[24] J.T. Munday, D.F. Bagster, A new ejector theory applied to steam jet refrigeration, Ind. Eng. Chem. Process Des. Dev. 16 (1977) 442–449.
[25] R. Hilsch, The use of the expansion of gases in a centrifugal field as cooling process, Rev. Sci. Instrum. 18 (1947) 108.
[26] B. Mun, D. Lee, Understanding morphology-controlled synthesis of Zinc nanoparticles and their characteristics of hydrolysis reaction, Langmuir 29 (2013) 6174–6180.
[27] SMPS 3936, Scanning Mobility Particle Sizer™, (SMPS™), Spectrometer; Operation and Service Manual, 2010 http://www.google.co.kr/url?sa=t&rct=j&q=&esrc=s&source=web&cd=1&ved=0ahUKEwiH_d7P6c_PAhWJQY8KHeTtDlMQFggcMAA&url=http%3A%2F%2Fcires.colorado.edu%2Fjimenez-group%2FManuals%2FSMPS_manual&usg=AFQjCNGTUdtDCxBu4m5-_tct5PyFKiXO9g&bvm=bv.135258522,d.c2I/.
[28] ASHRAE Position Document on Filtration and Air Cleaning, 2015. https://webcache.googleusercontent.com/search?q=cache:iRTuOiUggawJ:https://www.ashrae.org/File%2520Library/docLib/About%2520Us/PositionDocuments/ASHRAE-Position-Document-on-Filtration-and-Air-Cleaning.pdf+&cd=1&hl=ko&ct=clnk&gl=kr/.